

Accepted for publication in the Astrophysical Journal

A High Resolution X-ray Image of the Jet in M 87

H.L. Marshall¹, B.P. Miller¹, D.S. Davis¹, E.S. Perlman^{2,3}, M. Wise¹, C.R. Canizares¹, and D.E. Harris⁴

hermanm@space.mit.edu, brendan@mit.edu, dsd@space.mit.edu, perlman@umbc.edu,
wise@space.mit.edu, crc@space.mit.edu, harris@head-cfa.harvard.edu

ABSTRACT

We present the first high resolution X-ray image of the jet in M 87 using the *Chandra* X-ray Observatory. There is clear structure in the jet and almost all of the optically bright knots are detected individually. The unresolved core is the brightest X-ray feature but is only 2-3 times brighter than knot A (12.3'' from the core) and the inner knot HST-1 (1.0'' from the core). The X-ray and optical positions of the knots are consistent at the 0.1'' level but the X-ray emission from the brightest knot (A) is marginally upstream of the optical emission peak. Detailed Gaussian fits to the X-ray jet one-dimensional profile show distinct X-ray emission that is not associated with specific optical features. The X-ray/optical flux ratio decreases systematically from the core and X-ray emission is not clearly detected beyond 20'' from the core. The X-ray spectra of the core and the two brightest knots, HST-1 and A1, are consistent with a simple power law ($S_\nu \propto \nu^{-\alpha}$) with $\alpha = 1.46 \pm 0.05$, practically ruling out inverse Compton models as the dominant X-ray emission mechanism. The core flux is significantly larger than expected from an advective accretion flow and the spectrum is much steeper, indicating that the core emission may be due to synchrotron emission from a small scale jet. The spectral energy distributions (SEDs) of the knots are well fit by synchrotron models. The spectral indices in the X-ray band, however

¹Center for Space Research, Massachusetts Institute of Technology, 77 Massachusetts Ave., Cambridge, MA 02139

²Dept. of Physics, University of Maryland-Baltimore County, 1000 Hilltop Circle, Baltimore, MD 21250

³Dept. of Physics and Astronomy, Johns Hopkins University, 3400 North Charles St, Baltimore, MD 21218

⁴Harvard-Smithsonian Center for Astrophysics, 60 Garden St., Cambridge, MA 02138

are comparable to that expected in the Kardashev-Pacholczyk synchrotron model but are much flatter than expected in the pitch angle isotropization model of Jaffe and Perola. The break frequencies derived from both models drop by factors of 10 – 100 with distance from the core.

Subject headings: Galaxies: individual (M 87) – galaxies: jets – X-Rays: Galaxies

1. Introduction

The Chandra X-ray Observatory is now resolving the X-ray spatial structure along jets of radio galaxies and quasars. The jets of Cen A (Kraft et al. 2000), 3C 273 (Marshall et al. 2001), and PKS 0637-752 (Schwartz et al. 2000) are just three examples of how *Chandra* can be used to image jets at low to moderate redshifts. In the 3C 273 and PKS 0637-752 jets, the X-ray power dominates the spectral energy distributions (SEDs) of some of the jet knots and simple synchrotron and synchrotron self-Compton models can be ruled out directly. These quasars show superluminal motion in the radio-bright cores on scales of ~ 100 pc, which supports the possibility that the large scale jets at $\gtrsim 50$ kpc may also be moving superluminally, as required by a model where the X-ray emission results from inverse Compton scattering of the cosmic microwave background photons, such as suggested by Celotti, et al. (2001). There is no direct evidence, however, for superluminal motion on such large scales.

The M 87 jet is $\gtrsim 30''$ long and shows significant details in the optical and radio bands that differ only at the $\sim 0.1''$ level (Sparks et al. 1996). Superluminal motion is observed upstream of knot A (Biretta, Sparks, & Macchetto 1999) which is just under a kpc from the core. Previous X-ray observations by Schreier et al. (1980), Biretta, Stern, & Harris (1991), and Harris et al. (1997) detected the jet and ascribed most of its emission to knot A, the brightest knot at optical and radio wavelengths, so the M 87 jet offers a chance to test the background upscattering model. Böhringer et al. (2001) used the *XMM-Newton* telescope to resolve the core from knot A and show that their spectra were similar but the spatial resolution of none of the previous X-ray telescopes, including *XMM-Newton*, were sufficient to resolve the jet into more than one knot. The emission from the core is also of considerable interest for modelling of a possible advective accretion flow (Reynolds et al. 1996; Di Matteo et al. 2000).

We present the first X-ray images with sufficient resolution to identify and measure the X-ray emission from many knots in the jet. We then produce SEDs for each distinct knot in the jet and obtain X-ray spectra for several of these.

2. Observations and Analysis

M 87 was observed with the *Chandra* High Energy Transmission Grating Spectrometer (HETGS) on 2000 July 17-18 (JD - 2450000 = 1743.17-1743.64). The exposure time was 38048 s. The readout detector was the Advanced CCD Imaging Spectrometer (ACIS), which was read out in the timed exposure mode with 3.2 s frame times. The dispersed spectra of the core and knots were statistically poor and showed no apparent emission lines so we ignored them for the purposes of this work. All remaining analyses concerned only the image from the HETGS zeroth order. The zeroth order images are not affected by pileup because of the low count rates (< 0.1 count per frame) so point sources should be nearly Gaussian with a one dimensional standard deviation of about 0.32" (0.75" FWHM) (Marshall et al. 2001). At a distance of 16 Mpc (Tonry 1991), 1" is 78 pc.

Figure 1 shows the X-ray image binned in 0.2" pixels and adaptively smoothed. For comparison, images from the VLA and HST are also shown, taken from observations reported by Perlman et al. (2001a). Qualitatively, the X-ray emission from the jet is much brighter near the core compared to the optical emission. Knot HST-1 is the best example of the difference, being the second brightest knot in the X-ray image but it is the faintest of the knots optically. By way of contrast, X-ray emission is barely detectable beyond knot B, which is about 14" from the core. The jet is nearly one-dimensional, so a profile is used for quantitative analysis (Fig. 2), derived by summing data in a 1.5" wide window at a position angle of -70.4°, which is defined by the center of knot A. The X-ray flux reaches the background level at 21" from the nucleus.

Gaussians were fitted to the knots in the one dimensional profile of the jet. The results of the fits are given in Table 1. There is definite X-ray emission that is not included in any of the fitted regions, which were restricted to the locations of optically emitting knots. In particular, there is significant X-ray emission between knots D and E that is not included in either of these fitting regions which we label “DX”. Similarly, there is a “bridge” of X-ray emission between knots A and B, which corresponds to a region downstream of knot A. The X-ray flux clearly drops more rapidly than the optical flux does in this downstream region; the X-ray emission we label as knot G is perhaps more closely associated with the downstream end of knot C, based on the image (Fig. 1).

The distance from the core to the peak of the X-ray emission of knot A is $12.34 \pm 0.02''$, which is within 0.1" of the distance derived from the HST data, $12.43 \pm 0.01''$ (see table 1). Previous estimates of this separation using X-ray images with lower angular resolution (Neumann et al. 1997; Böhringer et al. 2001) gave smaller values, about 11.5". These estimates were probably biased by the flux in the bright HST-1 and D knots. Indeed, we find that the centroid of the core, HST-1, and D knots is $11.66 \pm 0.02''$ from knot A, which is consistent

with the *ROSAT* and *XMM* results. Thus, although we also find that the X-ray emission of knot A is upstream of the peak optical emission by $0.09 \pm 0.03''$, the offset is significantly smaller than previously estimated. Other knots show less significant displacements.

We tested for cross-jet extent of knot A by fitting Gaussians to the cross-jet profiles of the core/HST-1 knot combination as well as to knot A itself. The standard deviations (FWHMs) are $0.371 \pm 0.009''$ ($0.872''$) for the core region and $0.439 \pm 0.016''$ ($1.032''$) for knot A, indicating that knot A is broader than the core. Assuming that the core image represents a point source, we estimate the intrinsic FWHM of knot A to be $0.55 \pm 0.07''$. In the optical images, this knot is $1.0''$ wide (Sparks et al. 1996), so we conclude that the X-ray emission is more concentrated than the optical emission from this knot in the cross-jet direction following the trend observed by Sparks et al. (1996) that the knot appears narrower in the UV than in the optical and radio bands.

Four regions were selected for X-ray spectral fitting using 0.5-7.5 keV data reprocessed by the Chandra X-ray Center using CIAO 2.0b and the most recent response matrices for ACIS chip S3. Results are given in Table 2. The reduced χ^2 values are all acceptable at the 95% confidence level. The spectral indices of all regions are consistent with indices found by Böhringer et al. (2001), who did not resolve knots HST-1 and D from the core. These indices are consistent with a single value of α of 1.46 ± 0.05 . We tested the pulse height spectra of most knots against the spectrum of the core in order to determine if the spectra changed shape. The core was defined as a region $1''$ in diameter placed to exclude most of the flux of the HST-1 knot. Smirnov two-sample tests showed that the spectra of all knots, including HST-1, were consistent with that of the core at the 90% confidence level. By contrast, the radio-optical spectral indices of these knots are 0.66-0.71 and the optical spectral slopes are in the range 0.65-0.90 (Perlman et al. 2001a).

Flux densities of several knot regions are given in Table 1, based on Gaussian fits to the one dimensional profile shown in Fig. 2. We find that the total jet power is 1.59 ± 0.07 times that of the core power in the 0.5-5.0 keV band. The unabsorbed 0.5-10 keV luminosity of the core is 4.4×10^{40} erg s $^{-1}$.

3. Discussion

The observed luminosity and spectral index of the unresolved core can be used to constrain models of the accretion emission. Reynolds et al. (1996) estimated that the X-ray flux, νS_ν , was about 1.6×10^{-12} erg s $^{-1}$ cm $^{-2}$ at 1 keV and $< 7 \times 10^{-12}$ erg s $^{-1}$ cm $^{-2}$ at 5 keV at resolutions of $4''$ and $200''$, respectively. Reynolds et al. argued that the expected X-ray

flux from an advective flow would be a factor of 10-100 smaller than the observed values and suggested that the core optical and X-ray emission would instead result from a jet. We find somewhat smaller fluxes of 6.0 and 3.0×10^{-13} erg s $^{-1}$ cm $^{-2}$ at 1 and 5 keV at a resolution of $0.5''$; these fluxes are still $\sim 10\times$ larger than the expected emission due to accretion. It is also significant, however, that the advective flow model proposed by Reynolds et al. (1996); Di Matteo et al. (2000) produce X-ray emission by thermal bremsstrahlung at a characteristic temperature of 2×10^9 K, giving an X-ray spectrum that would be much flatter than observed. The new X-ray observations indicate that the M 87 core is probably dominated by a jet in the X-ray band. This interpretation is supported by $10\ \mu$ measurements (Perlman et al. 2001b). It is important to remember, however, that this conclusion is model-dependent, relying on modelling of the emission from advective flows. Allen, Di Matteo, & Fabian (2000) used ASCA spectra to argue for a hard spectral component ($\alpha = 0.4$) which they associate with the core. Guainazzi & Molendi (1999) also argued for a hard component based on *Bep-poSAX* data for the inner $2'$ with a flux about $2\times$ smaller than found by Allen, Di Matteo, & Fabian (2000). The expected 5 keV flux in the Allen, Di Matteo, & Fabian (2000) model is a factor of 20 larger than our measurement, which indicates that the hard flux is extended, a conclusion also reached by Matsumoto (1998) in M 87 and by Loewenstein et al. (2001) for other ellipticals modelled by Allen, Di Matteo, & Fabian (2000).

With the high resolution of *Chandra*, we have measured the X-ray flux densities of the knots detected in HST images in order to construct reliable spectral energy distributions (SEDs) (Fig. 3) using radio and optical flux densities from Perlman et al. (2001a). We have applied the usual synchrotron formulae (Pacholczyk 1970) to the radio-optical portions of the SEDs for knots HST-1, D, A, and B, finding equipartition magnetic field values in the range 250 to $320\ \mu$ G and synchrotron luminosities of 10^{40-42} erg s $^{-1}$. The particle Lorentz factors required to produce X-rays in these fields are close to $\gamma \approx 3 \times 10^7$ and the synchrotron loss lifetimes are of order 3 to 10 years (for 10^{18} Hz and 10^{17} Hz, respectively). Biretta, Stern, & Harris (1991) obtained similar results for their synchrotron models and the lifetimes are consistent with observed X-ray variability time scales (Harris et al. 1997).

Following Perlman et al. (2001a), we fitted the SEDs of each knot to the Jaffe & Perola (1973) and Kardashev-Pacholczyk Kardashev (1962); Pacholczyk (1970) synchrotron models, labelled JP and KP, respectively. These models are described by Perlman et al.; briefly, the JP model involves isotropization of the electron pitch-angle distribution while the KP model does not. Continuous injection models (Heavens & Meisenheimer 1987) generally fail to fit the X-ray data, as shown by Perlman et al. They determined that this model might still apply to knot A if the X-ray emission region were $\sim 5\times$ smaller than the optical emission region. We find that the width of the X-ray emission from knot A is about half that of the optical emission, so the emission volume could indeed be as small as required for the

continuous injection model. These data are not sufficient, however, to test for the extremely small volumes required for this model to fit other knots. Now that the X-ray flux density for knot HST-1 is known, we find that it may also be effectively modelled with a continuous injection model.

Fig. 3 shows that the KP model can fit all knot SEDs reasonably well while the JP model fits the optical data of knot B poorly. The break frequencies are quite different for these two models for knots furthest from the core. Fig. 4 shows that the break frequency, ν_B , drops systematically with position along the jet after knot HST-1. We do not yet have a model that predicts this behavior. The KP and JP models predict specific spectral indices in the X-ray band. For the KP model, the spectral indices are nearly identical for all knots in the jet: 1.7-2.1; these values are systematically larger than the observed average of 1.46. The JP model, however, would result in X-ray spectral indices that are usually larger than 3.5, which is much steeper than observed. These two models are used for illustrative purposes, giving an indication of the difficulties encountered in global fitting which, in turn suggests the need for spatially stratified emission regions Perlman et al. (1999, 2001a).

Since inverse Compton (IC) models using synchrotron emission as seed photons fail by factors of hundreds (Neumann et al. 1997; Böhringer et al. 2001), either the field is significantly smaller than the equipartition value (Heinz & Begelman 1997) or the seed photons come from the cosmic microwave background (CMB), which would be seen in the jet frame to have an energy density augmented by the jet's Lorentz factor (Γ) squared. We have applied the formulation of Harris & Krawczynski (2001), who solve for the beaming parameters under the assumption of a synchrotron source with equipartition field. While this sort of beaming model provides acceptable solutions for some sources such as PKS 0637-752 (Celotti, et al. 2001), in the case of M 87 rather extreme conditions would be required. In particular, the angle of the jet to the line of sight would have to be less than 5° and the beaming factors would be in the range 10 to 45. Such models would conflict with our current understanding of both VLBI scale and arcsec scale studies which essentially concur that the angle to the line of sight is of order 20° and the Lorentz factors are of order a few (Biretta, Sparks, & Macchetto 1999). Our synchrotron model fits into this conventional interpretation; there may well be significant beaming in the kpc jet of M87 but we are not in a favored position to see the primary effects. In all IC models, the X-ray spectral slopes should be comparable to those in the radio band while we find that the X-ray spectra are significantly steeper, even for knots HST-1 and D where some beaming might be expected, based on the observation of superluminal motion (Biretta, Zhou, & Owen 1995; Biretta, Sparks, & Macchetto 1999). Thus, purely based on the X-ray spectral indices, IC models do not readily explain the X-ray data.

At such high spatial resolution, we begin to see that modelling will be complicated by comparing emission from regions that are not strictly co-spatial so that spatially stratified emission regions may be required. Perlman et al. (1999) suggested this model in order to reconcile the radio and optical polarization vectors. Particle acceleration in the knots is required in order to replenish the supply of X-ray emitting electrons so the highest energy electrons will emit in the X-ray band and have the shortest lifetimes while the lower energy electrons can radiate further down the jet. We observe X-ray emission upstream of knot E, and that knot A appears closer to the core in the X-ray band than in the optical or radio bands. Our estimates of the synchrotron lifetimes of the X-ray emitting electrons – 3-10 yr – are consistent with the marginally significant offset we observe between the optical and X-ray positions of knot A: ~ 8 pc, given uncertainties in the angle of the jet to the line of sight and the bulk motion of the jet. For Cen A, which is $5\times$ closer, there are much clearer offsets (Kraft et al. 2000, 2001), resulting from particle diffusion and energy loss. Similarly, we may be observing lateral diffusion of shock-accelerated electrons in the cross-jet leading edge of knot A. The X-ray emission region would, again, be significantly smaller than the optical emission region. Higher resolution X-ray observations of the M 87 jet may well show morphological differences that will require somewhat more complex spectral modelling.

We thank Ralph Kraft for communicating results from *Chandra* observations of Cen A in advance of publication. This research is funded in part by NASA contracts NAS8-38249, and SAO SV1-61010. ESP was funded by NASA grant NAG5-9997 and HST grant GO-7866 and DEH was supported under grant NAS8-39073.

REFERENCES

Allen, S. W., Di Matteo, T., & Fabian, A. C. 2000, MNRAS, 311, 493
Biretta, J. A., Sparks, W. B., and Owen, F. N. 1995, ApJ, 520, 621
Biretta, J. A., Sparks, W. B., and Macchetto, F. 1999, ApJ, 520, 621
Biretta, J. A., Stern, C. P., and Harris, D. E. 1991, AJ, 101, 1632
Böhringer et al. 2001, A&A, 365, L181
Celotti, A., Ghisellini, G., and Chiaberge, M. 2001, MNRAS, 321, L1.
Di Matteo, T., Quataert, E., Allen, S. W., Narayan, R., & Fabian, A. C. 2000, MNRAS, 311, 507

Guainazzi, M. & Molendi, S. 1999, A&A, 351, L19

Harris, D. E., Biretta, J. A., and Junor, W. 1997, MNRAS, 284, L21

Harris, D. E. H. & Krawczynski, H. 2001, ApJ, submitted

Heavens, A. & Meisenheimer, K. 1987, MNRAS, 225, 335

Heinz, S. & Begelman, M. 1997, ApJ, 490, 653

Jaffe, W. J. & Perola, G. C. 1973, A&A, 26, 421

Kardashev, N. S. 1962, Soviet Astronomy – AJ, 6, 317

Kraft, R. P. et al. 2000, ApJ, 531, L9

Kraft, R. P. et al. 2001, ApJ, submitted

Loewenstein, M., Mushotzky, R. F., Angelini, L., Arnaud, K. A., & Quataert, E. 2001, ApJ, 555, L21

Marshall et al. 2001, ApJ, 549, L167

Matsumoto, H. 1998, Ph.D. thesis, Kyoto University

Neumann, M. Meisenheimer, K. Röser, H.-J., and Fink, H. H. 1997, A&A, 318, 383

Pacholczyk, A. G. 1970, Radio Astrophysics (San Francisco: Freeman)

Perlman, E. S., Biretta, J. A., Sparks, W. B., Macchetto, F. D., and Leahy, J. P. 2001a, ApJ, 551, 206

Perlman, E. S., Sparks, W. B., Radomski, J., Packham, C., Biretta, J. A., and Fisher, R. S. 2001b, ApJ, submitted

Perlman, E. S., Biretta, J. A., Zhou, F., Sparks, W. B., and Macchetto, F. D. 1999, AJ, 117, 2185

Reynolds, C. S., Di Matteo, T., Fabian, A. C., Hwang, U., & Canizares, C. R. 1996, MNRAS, 283, L111

Schreier, E. J., Gorenstein, P., and Feigelson, E. D. 1980, ApJ, 261, 42

Schwartz et al. 2000, ApJ, 540, L69

Sparks, W. B., Biretta, J. A., and Macchetto, F. 1996, ApJ, 473, 254

Tonry, J. L. 1991, ApJ, 373, L1

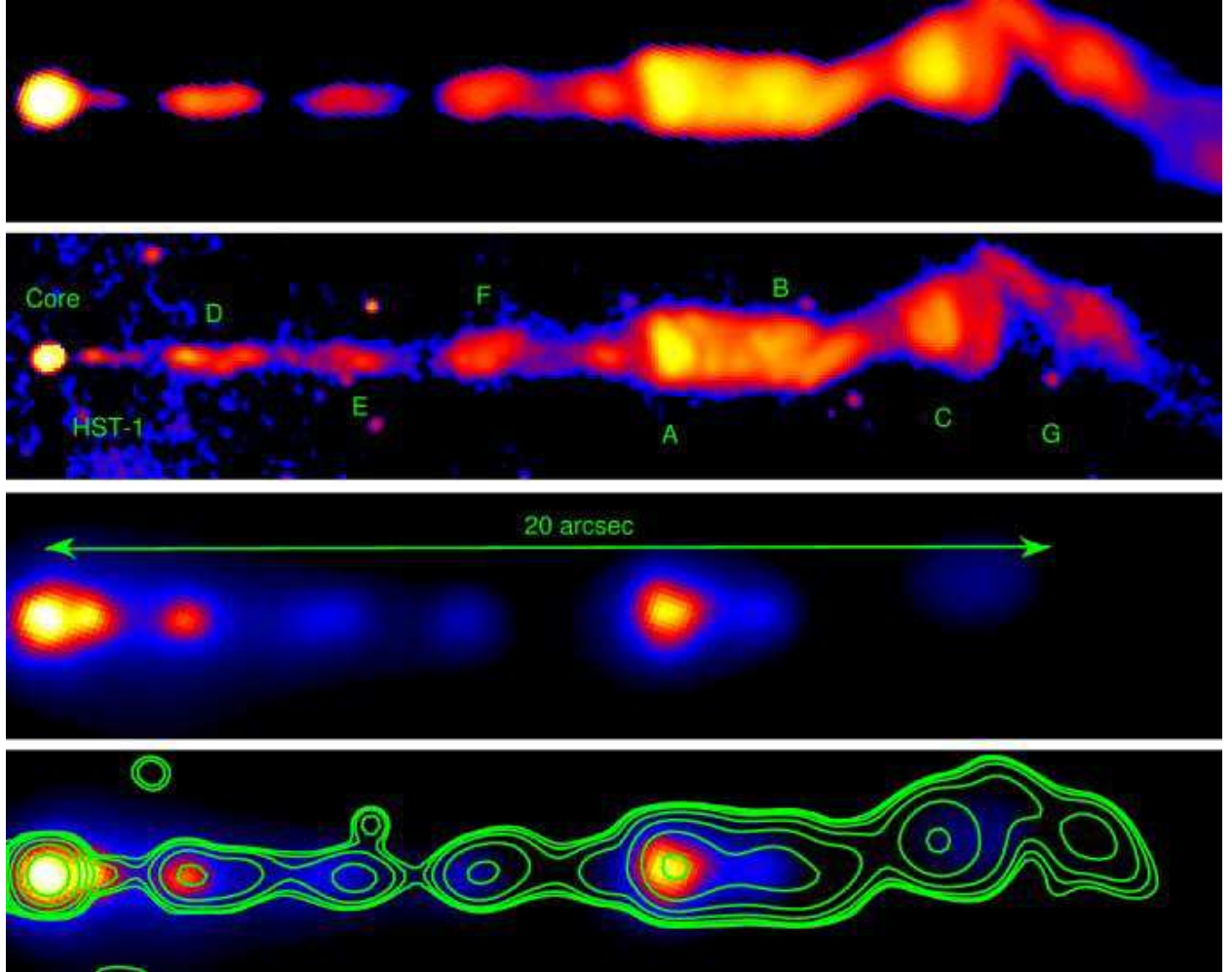


Fig. 1.— Images of the jet in M 87 in three different bands, rotated to be horizontal, and an overlay of optical contours over the X-ray image. *Top*: Image at 14.435 GHz using the VLA. The spatial resolution is about $0.2''$. *Second panel*: The *Hubble Space Telescope Planetary Camera* image in the F814W filter from Perlman et al. (2001a). The brightest knots are labelled according to the nomenclature used by Perlman et al. (2001a) and others. *Third panel*: Adaptively smoothed *Chandra* image of the X-ray emission from the jet of M 87 in $0.20''$ pixels. The X-ray and optical images have been registered to each other to about $0.05''$ using the position of the core. *Fourth panel*: Smoothed *Chandra* image overlaid with contours of a Gaussian smoothed version of the HST image, designed to match the *Chandra* point response function. The X-ray and optical images have been registered to each other to about $0.05''$ using the position of the core. The HST and VLA images are displayed using a logarithmic stretch to bring out faint features while the X-ray image scaling is linear.

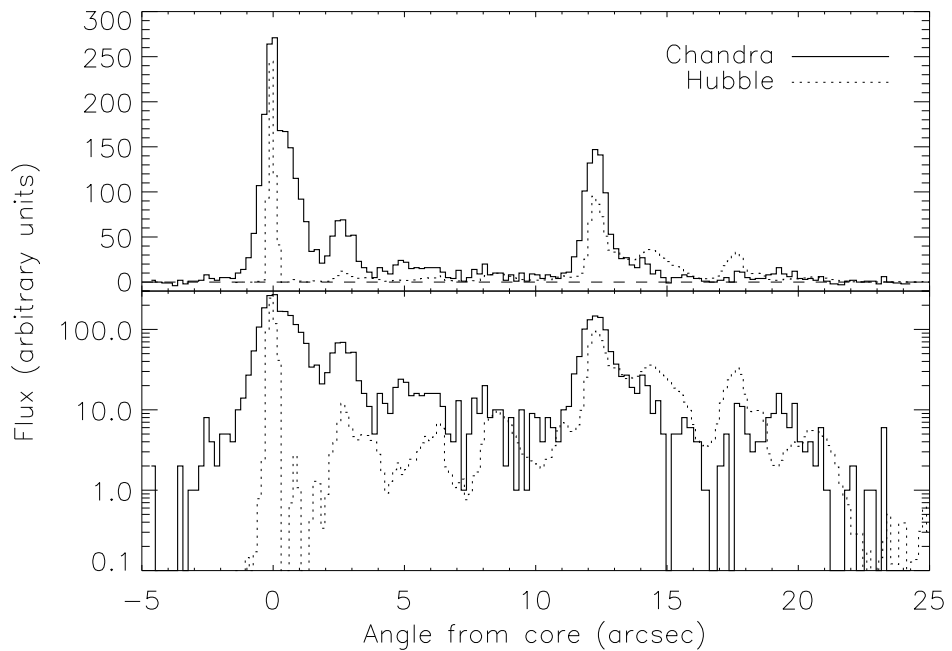


Fig. 2.— Profiles of the M 87 jet in the X-ray (solid, in counts per $0.2''$ bin) and optical bands (dashed) using the images shown in Fig. 1. The optical data were scaled such that 28.4 nJy per $0.152''$ bin corresponds to a vertical value of 200. With logarithmic scaling (bottom panel), it is very clear that the X-ray fluxes decrease relative to the optical flux with increasing angle from the core.

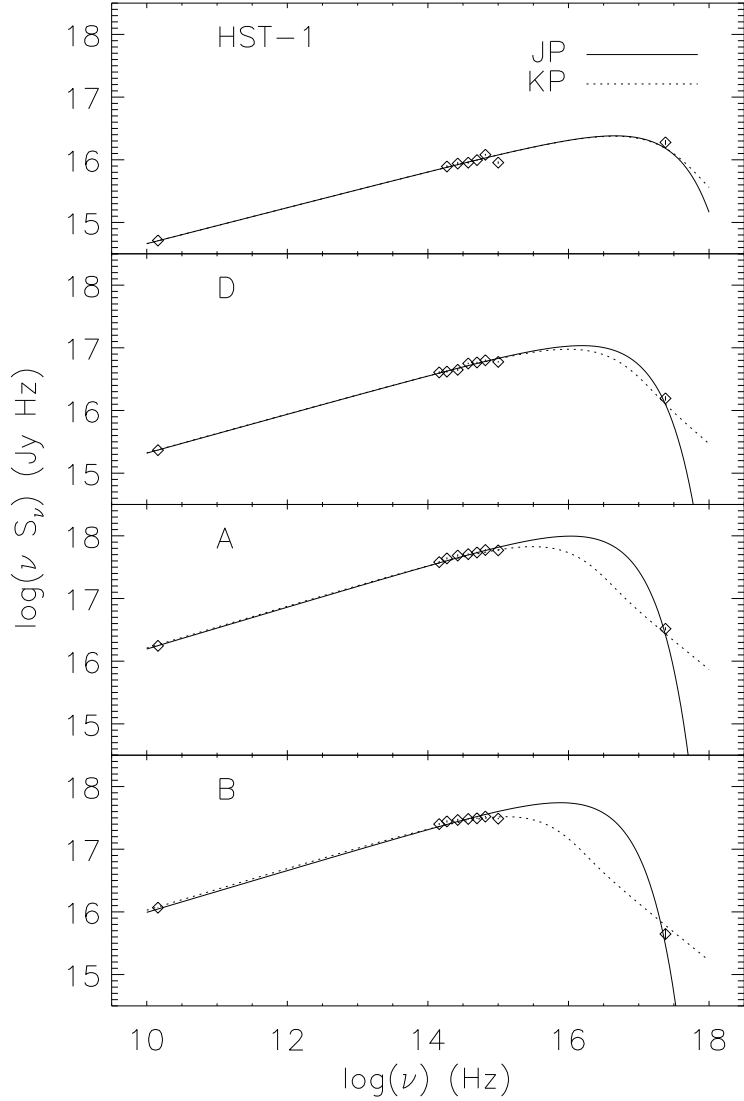


Fig. 3.— The spectral energy distributions (SEDs) of the M 87 jet knots. Error bars are given for each data point and are usually much smaller than the plot symbols. There is clear evidence of spectral steepening in the optical-UV data for knots A and B but a stronger break or cutoff is required to fit the X-ray flux density. The data were fitted to Jaffe & Perola (1973) and Kardashev-Pacholczyk Kardashev (1962); Pacholczyk (1970) synchrotron models, shown as dotted and dashed lines, respectively. The KP model can fit all knot SEDs reasonably well while the JP model fits the optical data of knot B poorly. The break frequencies obtained for the outlying knots are quite different for these two models; see also Fig. 4.

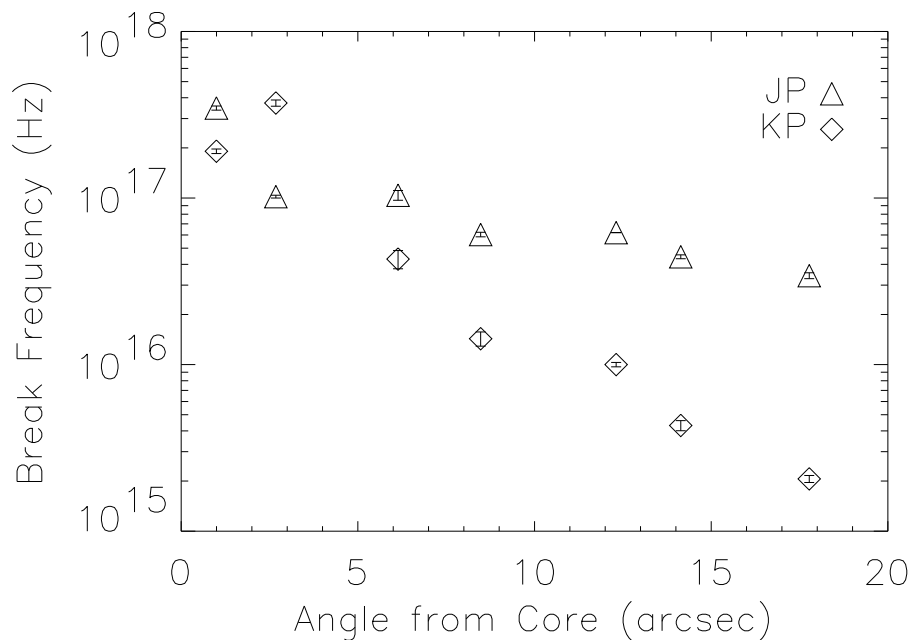


Fig. 4.— Synchrotron break frequency from fits to the spectral energy distributions of each knot, as shown in Fig.3. The JP and KP synchrotron models are taken from Jaffe & Perola (1973) and Kardashev (1962); Pacholczyk (1970), respectively. Note the systematic downward trend of the break frequencies.

Table 1. Flux Densities and Positions^a of Knots in the M 87 Jet

Feature	θ_x ($''$)	S_ν ^b (nJy)	θ_o ($''$)	θ_r ($''$)
Core	0.00	245 ± 10	0	0
HST-1	1.02 ± 0.03	82 ± 7	0.92	1.16
D ^c	2.71 ± 0.03	67.9 ± 5.6	2.79	3.09
DX ^c	4.93 ± 0.05	21.1 ± 3.5
E	6.16 ± 0.06	15.4 ± 3.1	6.15	5.98
F	8.50 ± 0.08	10.0 ± 2.6	8.65	8.71
A	12.34 ± 0.02	142 ± 8	12.43	12.49
B	14.16 ± 0.06	19.2 ± 3.5	14.45	14.44
C	17.80 ± 0.10	7.2 ± 2.5	17.70	17.69
G ^d	19.33 ± 0.07	11.6 ± 2.7

^aPositions are given as angular distances from the core in units of arcsec for the X-ray, optical, and radio bands, as designated by the subscript on θ . The systematic uncertainties in the optical and radio values are estimated to be about $0.01''$.

^bFlux density at 1 keV assuming a spectral index of 1.46, the uncertainty weighted average of values from table 2.

^cThe X-ray flux of knot D is spatially associated with the optical emission of knot D-east, as defined by Perlman et al. (1999) while Knot DX is not clearly associated with any of the D subknots found in HST images.

^dThe X-ray emission appears to be more closely related to the end of knot C rather than knot G based on the position angle.

Table 2. Power Law Spectral Fits for Knots in the M 87 Jet

Region	α^a	χ^2 (dof) ^b
Core & HST-1	1.47±0.08	1.19 (61)
Knot HST-1	1.29±0.14	0.93 (22)
Knot D	1.33±0.17	1.53 (22)
Knot A	1.57±0.10	1.12 (32)

^aUncertainties are 90% confidence values for 1 interesting parameter for a power law of the form $S_\nu \propto \nu^{-\alpha}$, with the column density of interstellar gas fixed to $2.5 \times 10^{20} \text{ cm}^{-2}$

^bReduced χ^2 for the number degrees of freedom given in parentheses